Bogdanović-Jovanović, J. B., *et al.*: Performance of Low-Pressure Fans …
THERMAL SCIENCE, Year 2016, Vol. 20, Suppl. 5, pp. S1435-S1447

S1435

PERFORMANCE OF LOW-PRESSURE FANS
OPERATING WITH HOT AIR

by

Jasmina B. BOGDANOVIĆ-JOVANOVIĆ[a], Dragica R. MILENKOVIĆ[a],*
Živan T. SPASIĆ[a], and Dragan M. SVRKOTA[b]

[a] Faculty of Mechanical Engineering, University of Nis, Nis, Serbia
[b] Jaroslav Cerni Institute for the Development of Water Resources, Belgrade, Serbia

Performance characteristics of fans are generally provided for the normal temperature and pressure conditions ($t_I = 20\ °C$, $p_I = 101.325\ kPa$, $\rho_I = 1.2\ kg/m^3$). Very often, fans operate in different air conditions, occasionally at different air temperatures. In these cases, equations obtained by the law of similarity are usually used for recalculation of the fan operating parameters. Increasing the inlet air temperature causes a decrease in the characteristic of Reynolds number, and may lead to efficiency lowering of the fan. There are also some empirical formulas for recalculation of fan efficiency, when operating at different air temperatures. In this paper, the common way for obtaining fan performance for different operating conditions (air temperature changing) is presented. The results, obtained by recalculation of fan parameters using a law of similarity, are compared to numerical simulation results of the axial-flow fan operating with different air temperatures. These results are compared with results obtained by some recommended empirical formulas, as well. This paperwork is limited to low-pressure and mid-pressure fans, which represents the majority of all fans used in practice, for different purposes.

Key words: *low pressure and medium pressure fans, performance characteristics, air temperature, energy efficiency*

Introduction

Fans, as machines that utilize the mechanical energy of a rotating impeller to produce both movement of the air and an increase of the total pressure, are widely used in various spheres of life and work. Mainly their application is in air-cooling of all kind of electrical appliances, regardless of their size. Fans operate as the basics equipment for ventilation and air conditioning, regardless of whether it is a small open area or the entire underground mine. Industrial fan application is indispensable, considering that various technological processes include implementation of fans (such as drying, cooling, *etc.*). In industrialized countries, up to 10% of the total electrical energy consumption is used for the fan operation, showing the importance of improving fan operation and increasing their energy efficiency [1]. In practice, the most commonly are used low-pressure and mid-pressure fans, where the changing of air density can be neglected. Concerning the large use of low-pressure and mid-pressure fans, it's highly desirable to operate in economic regimes, which represents the area of fan performance

_____

∗ Corresponding author: bminja@masfak.ni.ac.rs

S1436

Bogdanović-Jovanović, J. B., *et al.*: Performance of Low-Pressure Fans …
THERMAL SCIENCE, Year 2016, Vol. 20, Suppl. 5, pp. S1435-S1447

curve where fan achieves a minimum of 80% of its maximum efficiency level, so-called best efficiency point, or (BEP) [2]. From the standpoint of energy efficiency, operating regimes of fan close to the BEP is of the greatest importance in cases where fan operates a large number of working hours per day or even continuously. Therefore, even a small decrease of fan efficiency, can create large costs of electrical energy. To this day many books and papers on fan designing methods and their performance characteristics have been published [1-5]. Numerous experimental investigations of fan performances, using different measuring techniques, have been carried out, with the objective to improve fan design methods and to increase fan efficiency [6-8]. Design methods are constantly improving by using modern CFD techniques for numerical simulations of fluid flow in fan runners [9-14]. Thus, the modern research of turbomachinery in general, fan as well, represents the theory, experimental, and numerical investigations trinity.

Low-pressure and mid-pressure fan operating characteristics

It can be considered that the Mach numbers at the fan inlet and outlet flow, for low-pressure and mid-pressure fans, are smaller than 0,5. Developing the ratio of total (p_t) and static pressure (p_s) into the series by Mash number, $p_t/p_s = (T_t/T_s)^{\kappa/\kappa-1} = 1 + (\kappa - 1)\mathrm{Ma}^2/2 + \dots$ [1], at inlet and outlet cross-sections of the fan, the relation between total and static pressure can be formulate by the following equation

$$p_t = p_s + 0,5\rho c^2 \qquad (1)$$

For incompressible fluid (ρ = const.), with an error less than 1% [1]. The second term of the right side of the eq. (1) represents the dynamic pressure.

Volumetric flow rate of the fan, Q, is equal to the volume flow at the inlet, therefore:

$$Q = Q_I = c_I A_I \qquad (2)$$

where c_I is the averaged flow velocity at the fan inlet, and A_I is the flow area of the fan inlet.

Total pressure of the fan ($\Delta p_{t.f}$) is defined as the difference between the total pressure at the outlet (II) and total pressure at the inlet (I) cross-sections of the fan:

$$\Delta p_{t.f} = p_{t.II} - p_{t.I} \qquad (3)$$

If A_{II} is the flow area of the fan outlet, the dynamic pressure of the fan is defined as the dynamic pressure at the outlet cross-section of the fan:

$$p_{d.f} = p_{d.II} = 0,5\rho_{II} c_{II}^2 = 0,5\rho_{II}\left(\frac{Q_{II}}{A_{II}}\right)^2 \qquad (4)$$

For low-pressure ($\Delta p_{t.f} \leq 1$ kPa) and mid-pressure fans ($\Delta p_{t.f} \leq 3$ kPa), gas density changes in the fan can be neglected ($\rho_I = \rho_{II}$, $Q_{II} > Q$), therefore:

$$p_{d.f} = 0,5\rho_I\left(\frac{Q}{A_{II}}\right)^2, \quad \text{for } \Delta p_{t.f} \leq 3 \text{ kPa} \qquad (4a)$$

The total pressure of high-pressure centrifugal fans goes up to 13 kPa, causing an increase of air density in the fan about 10% ($\rho_{II}/\rho_I \leq 1, 1$).

Bogdanović-Jovanović, J. B., *et al.*: Performance of Low-Pressure Fans …
THERMAL SCIENCE, Year 2016, Vol. 20, Suppl. 5, pp. S1435-S1447

S1437

Due to relatively small pressure increase in the fan, and due to the relatively small gas density change in the fan, the gas density change can be calculated, with a negligible error, according to the isentropic law $\rho_{II} = \rho_I (p_{II}/p_I)^{1/\kappa}$, therefore, eq. (4) becomes:

$$p_{d.f} = 0,5\rho_I \left(\frac{Q_{II}}{A_{II}}\right)^2 \frac{1}{\beta_d}, \quad \text{where } \beta_d = \left(\frac{p_{II}}{p_I}\right)^{1/\kappa} \tag{5}$$

and $\beta_d \geq 1$ is the correction factor due to compressibility of the gas (air).

For the low-pressure fans $\beta_d \leq 1,007$, and for the mid-pressure fans $\beta_d \leq 1,007$, thus, in the cases of these fan types, the eq. (4a) can be used [1].

For the suction loaded fans, the relevant operating parameter is the static pressure of the fan, $p_{s.f}$, which is defined as the difference between total and dynamic fan pressure,

$$p_{s.f} = \Delta p_{t.f} - p_{d.f} \tag{6}$$

The fan power, N, is the power obtained on the fan shaft, and effectively used fan power, N_{ef}, can be calculated using [1]:

$$N_{ef} = \beta Q \Delta p_{t.f} \tag{7}$$

where

$$\beta = \frac{\kappa}{\kappa-1}\frac{1}{\Pi_t - 1}\left(\Pi_t^{\frac{\kappa-1}{\kappa}} - 1\right), \quad \text{and } \Pi_t = \frac{p_{t.II}}{p_{t.I}} = 1 + \frac{p_{t.f}}{p_{t.I}} \tag{7a}$$

The coefficient β $(\beta \leq 1)$ takes into account the compressibility of the gas.

For low-pressure and mid-pressure fans $\beta = 1$, and $0,99 > \beta > 0,95$ for high-pressure fans (3 kPa $\leq \Delta p_{t.f} \leq$ 13kPa, $1,03 < \Pi_t < 1,13$) [1].

Fan efficiency, η, is the ratio of the effectively used power and the actual fan power:

$$\eta = \frac{N_{ef}}{N} = \beta\frac{Q\Delta p_{t.f}}{N} \tag{8}$$

Using the analogy, the static fan efficiency, η_s, is defined:

$$\eta_s = \frac{\beta Q p_{s.f}}{N}, \quad (\eta_s < \eta) \tag{9}$$

The static efficiency of the fan defined as in eq. (10) does not give a realistic assessment of the quality of the transformed of energy in the fan, since it excludes mechanical energy from the dynamic pressure of the fan.

Operating characteristics (operating curve) of the fan represents functional relationships $\Delta p_{v.f}(Q)$, $p_{s.f}(Q)$, $N(Q)$, $\eta_s(Q)$, and $\eta(Q)$, usually given in the form of the graphic.

Operating characteristics of the fan is obtained experimentally, in the normal air conditions ($t_I = 20\ ^oC$, $p_I = 101.325$ kPa, $\rho_I = 1.2$ kg/m^3). Using the similarity law, these operating parameters can be recalculated for different flow parameters and different number of revolution of the fan, as well as for the different gas density at the inlet cross-section of the fan. Air density is obtained by the Clapeyron equation $\rho = p/(RT) = p/(288T)$.

Denoting with 1 and 2 an average geometric and flow parameters at the fan inlet and the fan outlet, respectively, the specific work of the fan runner, and pressure rise in the fan runner, is calculated using the Euler's equation for turbomachinery:

$$Y_k = \omega[(rc_u)_2 - (rc_u)_1], \quad i.\ e.\quad \Delta p_k = \rho\omega[(rc_u)_2 - (rc_u)_1] \tag{10}$$

where ω is the angular velocity of the fan runner, c_{1u} and c_{2u} – the circumferential components of the absolute flow velocity at fan inlet and outlet cross-sections.

In theory of turbomachinery, the usual assumption is that the entrance into the fan runner (cross-section 1) is slightly in front of the fan runner, and that the outlet (cross-section 2) is slightly behind of the fan runner. For fans designed without the guide vanes in front of the fan runner, $c_{1u} = 0$ (fans with non-swirl flow condition at the inlet), eq. (10) become:

$$Y_k = \omega(rc_u)_2 = 0,5\omega D c_{u2}, \quad and \quad \Delta p_k = 0,5\rho\omega D c_{u2} \tag{11}$$

where D is the characteristic diameter of the fan (the outer diameter).

The pressure of the fan runner Δp_k is greater than the total pressure of the fan, $\Delta p_{t.f}$, for the value of the total pressure loss in the fan ($\Delta p_{t.1-2}$):

$$\Delta p_k = \Delta p_{t.f} + \Delta p_{t.I-II} \tag{12}$$

The hydraulic fan efficiency is defined as a relation between the total pressure of the fan and the pressure of the fan runner (*i. e.* actual and effective power of the fan):

$$\eta_h = \frac{\Delta p_{t.f}}{\Delta p_k} = 1 - \frac{\Delta p_{t.I-II}}{\Delta p_k} \tag{13}$$

The total pressure loss in the fan due to viscous friction can be calculated:

$$\Delta p_{t.I-II} = K_{I-II}^{(p)} Q^2 \tag{14}$$

where $K_{I-II}^{(p)}$ [Pa(m^{-3}s^{-1})$^{-2}$] is the coefficient of total pressure loss in the fan.

Coefficient $K_{I-II}^{(p)}$ depends on fan geometric parameters (taking into account the roughness of the walls of the current channel) and the Reynolds number, as the characteristics of turbulent flow in the fan. In the case where the coefficient $K_{I-II}^{(p)}$ does not depend on Reynolds number, the fluid flow in the fan has automodel conditions by Reynolds numbers.

It is shown [1-5] that, for $\rho \approx$ const., the fan efficiency is equal to the product:

$$\eta = \eta_m \eta_Q \eta_h \tag{15}$$

where η_m, η_Q, and η_h are the mechanical, volumetric and hydraulic fan efficiency, respectively:

$$\eta_m = \frac{N_k}{N} \quad and \quad \eta_Q = \frac{Q}{Q_k} = 1 - \frac{\Delta Q}{Q_k} \tag{15a}$$

where Q_k is the volumetric flow rate in the fan runner ($Q_k = Q + \Delta Q$), ΔQ – the flow losses in the fan runner, N_k is the power of the fan runner ($N_k = \rho Q_k Y_k = Q_k \Delta p_k$).

All fan quantities used in the paper are defined by equations from the previous section [1].

**Reynolds number influence
on fan efficiency**

Reynolds number, as the characteristics of turbulence intensity in the fan, is defined by the following formula:

$$\mathrm{Re}\,u = u\frac{D}{\nu} = \frac{\pi D^2 n}{60\nu}, \quad n\,[\min^{-1}] \tag{16}$$

where u is the circumferential velocity, D – the fan diameter, ν – the coefficient of kinematic viscosity of the air.

Density and kinematic viscosity of the air depend on the air temperature, for the normal air pressure condition ($p = 101325$ Pa), as shown in tab. 1.

From tab. 1 one can conclude that with increasing the temperature, at constant pressure, the air density decreases, and the kinematic viscosity increases. Due to the kinematic viscosity increase, at constant speed fans, Reynolds number of the fan decreases. In the flow in automodel field by Reynolds numbers, fan efficiencies are equal.

For $\mathrm{Re}\underline{u} < \mathrm{Re}u^{(\mathrm{cr})}$ air flow in fans are not in automodel field by Reynolds numbers, and then fan efficiency depends on the value of the Reynolds number.

By examining 50 different centrifugal fans constructed in the Russian Institute CAGI [4] fig. 1 shows area of application of fan efficiencies as a func-

Table 1. Density and kinematic viscosity for air pressure $p = 101{,}3$ kPa

t [°C]	0	20	50	80	110
ρ [kgm^{-3}]	1.29	1.20	1.09	1	0.92
ν [m^{2}s^{-1}]	$1.33\cdot10^{-5}$	$1.5\cdot10^{-5}$	$1.8\cdot10^{-5}$	$2.06\cdot10^{-5}$	$2.4\cdot10^{-5}$
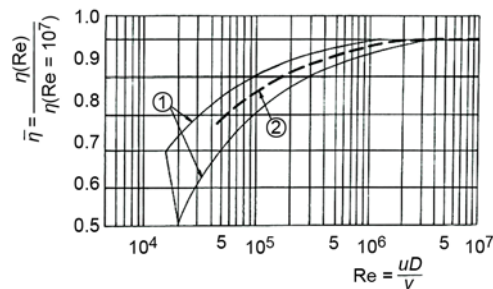
Figure 1. Influence of $\mathrm{Re}u$ number on the fan efficiency of centrifugal fans; *1 – the area of fan efficiency changing, due to experimental values [4], 2 – funcional graph, eq. (17) – averaged value of relative decreasing of fan efficiency*

tion Reynolds number, taking as a comparative fan efficiencies for $\mathrm{Re}u = 10^7$. In the same figure dotted line 2 shows the mean value and relative decrease of efficiency, according to which certain functions eq. (17) was obtained. According to fig. 1, $\mathrm{Re}u^{(\mathrm{cr})} = 10^7$, but in engineering practice is $\mathrm{Re}u^{(\mathrm{cr})} = 5\cdot10^6$.

Assuming a functional dependence $\bar{\eta}(\mathrm{Re}u)$ in the form $\bar{\eta} = 1 - a/\mathrm{Re}u^b$, and by defining the coefficients a and b using $\bar{\eta} = 0{,}99$ for $\mathrm{Re}u = 5\cdot10^6$ and $\bar{\eta} = 0{,}75$ for $\mathrm{Re}u = 5\cdot10^4$, the equation for centrifugal fans becomes:

$$\bar{\eta} = 1 - \frac{480}{\mathrm{Re}\,u^{0,7}}, \quad \text{for} \quad \mathrm{Re}\,u \geq 5\cdot10^4 \tag{17}$$

With regards to the eq. (17), the recalculation of efficiency can be done by using the following equation:

$$\eta' = \eta\frac{\bar{\eta}(\mathrm{Re}\,u')}{\bar{\eta}(\mathrm{Re}\,u)} = \eta F(\mathrm{Re}\,u, \mathrm{Re}\,u'), \quad \text{where} \quad F(\mathrm{Re}\,u, \mathrm{Re}\,u') = \frac{1 - \dfrac{480}{(\mathrm{Re}\,u')^{0,7}}}{1 - \dfrac{480}{\mathrm{Re}\,u^{0,7}}} \tag{18}$$

A fan efficiency reduction, for the same fan ($D' = D$) occurs when $\mathrm{Re}\,u' < \mathrm{Re}\,u^{(\mathrm{cr})}$:

S1440

Bogdanović-Jovanović, J. B., *et al.*: Performance of Low-Pressure Fans …
THERMAL SCIENCE, Year 2016, Vol. 20, Suppl. 5, pp. S1435-S1447

(1) When rotational speed of the fan is reduced below the critical value, $n' < n^{(\mathrm{cr})}$, where:

$$n^{(\mathrm{cr})} = \frac{60 \nu \, \mathrm{Re}\, u^{(\mathrm{cr})}}{\pi D^2}$$

(2) When, due to air temperature increasing, kinematic viscosity of the fan is reduced below the critical value, $\nu > \nu^{(\mathrm{cr})}$, where:

$$\nu^{(\mathrm{cr})} = \frac{\pi D^2 n}{60 \, \mathrm{Re}\, u^{(\mathrm{cr})}}$$

For recalculation of axial-flow fan efficiency, the equation of Stephenson [15] can be used, which is valid for $\mathrm{Re}\, u = 5 \cdot 10^4$:

$$\eta' = \eta + \frac{1,558}{\mathrm{Re}\, u^{0,2}} \left[1 - \left(\frac{\mathrm{Re}\, u}{\mathrm{Re}\, u'} \right)^{0,2} \right] \qquad (19)$$

There is also a universal formula for efficiency correction, given by Ackert [16], for both axial-flow fans and centrifugal fans, recomended (but not obligatory) in VDI and AMCA normas for fan testing:

$$\eta' = 1 - 0,5(1 - \eta) \left[1 + \left(\frac{\mathrm{Re}\, u}{\mathrm{Re}\, u'} \right)^{0,2} \right] \qquad (20)$$

Equation for fan operating regime conversion

According to the affinity laws of turbomachinery, particularly kinematic similarity of flow through the same fan ($D' = D$), the following equations for recalculation of operating regime for low-pressure and mid-pressure fans ($\rho \approx$ const., $\beta_d \approx 1$, $\beta \approx 1$) are obtained in forms:

$$Q' = Q \frac{n'}{n}, \qquad \Delta p_{\mathrm{t.f}}' = \Delta p_{\mathrm{t.f}} \frac{\rho_I'}{\rho_I} \left(\frac{n'}{n} \right)^2 \frac{\eta_h'}{\eta_h}, \qquad \eta' = \mathrm{f}(\eta) \qquad (21)$$

The following equations are joined to the equations (21):

$$N' = \frac{Q' \Delta p_{\mathrm{t.f}}'}{\eta'}, \qquad p_{\mathrm{s.f}}' = \Delta p_{\mathrm{t.f}}' - p_{\mathrm{d.f}}', \qquad \eta_s' = \frac{Q' p_{\mathrm{s.f}}'}{N'} \qquad (22)$$

Assuming $\eta_{\mathrm{m}} = \eta_{\mathrm{m}}'$ and $\eta_Q = \eta_Q'$, according to eq. (15) and, for example, eq. (18):

$$\frac{\eta_h'}{\eta_h} = \frac{\eta'}{\eta} = F(\mathrm{Re}\, u, \mathrm{Re}\, u') \qquad (23)$$

For the same number of revolutions, $n' = n$, the eqs. (21) become:

$$Q' = Q, \qquad \Delta p_{\mathrm{t.f}}' = \Delta p_{\mathrm{t.f}} \frac{\rho_I'}{\rho_I} \frac{\eta_h'}{\eta_h} = \Delta p_{\mathrm{t.f}} \frac{\rho_I'}{\rho_I} F(\mathrm{Re}\, u, \mathrm{Re}\, u'),$$

$$\eta' = f(\eta) = \eta F(\mathrm{Re}\, u, \mathrm{Re}\, u') \qquad (24)$$

When recalculating the operating fan regimes, with regard to the air density change, eq. (22) joins eqs. (24), as well. In addition, due to the Clapeyron equation, if the inlet pressure is the same $p_I' = p_I$, then $\rho_I'/\rho_I = T_I/T_I'$.

Numerical determination of low-pressure and mid-pressure fans operating regimes

As the example of a low-pressure fan is considered one low-pressure axial-flow fan, with seven blades, which is designed for cooling the car engine [12]. The fan has specific hub shape, which is extremely flat, due to the lack of space in which is mounted in.

Calculated operating parameters of the fan are: flow rate $Q = 1050$ m^3/h (= 0,292 m^3/s), therefore mass flow rate $\dot{m} = 0.350$ m^3/s, total pressure of the fan $\Delta p_{t.f} = 115$ Pa, rotational speed $n = 2600$ min^{-1} (*i. e.* n = 43.33 s^{-1}). A hub diameter is $D_i = 110$ mm and a shroud diameter is $D_e = 280$ mm. The fan width is only 38 mm, which causes an atypical, flat shape hub, which impairs its aerodynamics and fluid flow at the entrance to the fan impeller. Characteristic numbers are:

$$\varphi = \frac{Q}{A_e u_e} = \frac{4Q}{D_e^3 \pi^2 n} = 0,12, \quad \psi = \frac{2\Delta p_t}{\rho u_e^2} = \frac{2\Delta p_t}{\rho D_e^2 \pi^2 n^2} = 0,132, \quad n_q = 157,8\frac{\varphi^{1/2}}{\psi^{3/4}} = 249,6 \quad (25)$$

The ratio of internal and external diameter of the fan is $\bar{d} = D_i/D_e = 0,39$. For fans with fan runner only, $\bar{d} = 0,35 \div 0,40$, and a recommendation for the number of blades is within the limits $z = 4\text{-}8$ [5, 17]. In presented case, the fan is designed with seven blades.

Specified geometrical parameters (diameters and shapes hub) cause that the designed fan has a significantly lower efficiency compared to the maximum possible efficiency of this type of fan (fan runner only). Thus the expected maximum hydraulic efficiency of $\eta_h = 0.50$, and the total efficiency of $\eta = 0.47$.

Figure 2 shows the geometry of axial fan runner, designed in the software BladeGen. Measurements of fan operating parameters have been obtained on the test rig in the Laboratory of Hydraulic machines, in the Faculty of Mechanical Engineering Nis, Nis, Serbia. Since the test rig consists of the cylindrical test chamber (partly shown in fig.
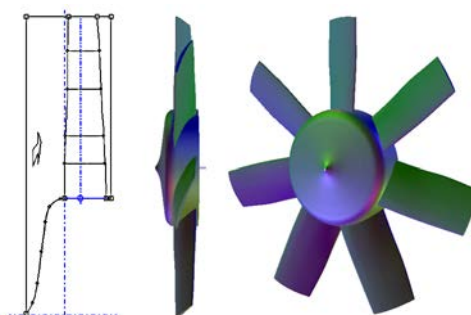

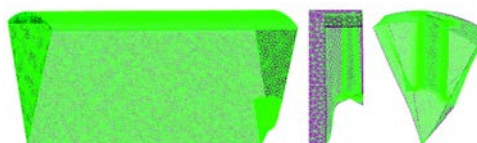**Figure 2. Geometry of the axial-flow fan**

Figure 3. Numerical mesh of the axial-flow fan in the measuring chamber

3), the numerical simulation geometry is made to be identical. Therefore, besides the fan, it was necessary to make the geometrical and numerical model of the test chamber as well, in order to simulate the working conditions of laboratory fan testing. The axial-flow fan is located in a cylindrical chamber (a diameter 800 mm and a length 800 mm), shown in figure 3.

For numerical simulations of fluid flow in axial-flow fan, the commercial code Ansys CFX was used, solving continuity equation and 3-D Reynolds-average Navier-Stokes equations. The standard $k\text{-}\varepsilon$ turbulent model is used, which has been considered optimal for

numerical simulations of turbomachinery [9, 18]. Due to axial symmetry of flow field, Ansys CFX software can be applied for just one blade area, *i. e.* one blade and a half of the space between both sides (for this particular axial-flow fan it is 1/7 of the fan runner).

The computational mesh, created in ICEM CFD 14.0 and Blade Generator software, is consists of 862144 elements (185007 nodes), of which 792100 are tetrahedrons and 70044 are prisms). Axial-flow fan contains 606061 elements and much larger measuring chamber 256083 elements. Obviously, the discretization mesh is unstructured, where the overlapping elements and elements in contact between two meshes are formed carefully, so that the transition larger to small elements is not too abrupt, fig. 3. The meshing is refined near the walls and around the blade. In the fan domain, the maximal value of *y+* is less than 100 and the averaged value of *y+* is less than 10 [18, 19]. Interpolation of values from the cell center to the cell faces are accomplished using the high-resolution scheme. The series of numerical simulations, for different mass flow rate at the inlet and referent atmospheric pressure at the fan outlet, are carried out. The convergence criteria for numerical simulations were that root mean square values of the equation residuals are 10^{-4}.

Table 2. Grid independence test results for Q = 0,246 m³/s, $\Delta p_{t.f}$ = 125 Pa, n = 2600 min⁻¹

Number of mesh elements	Total pressure $\Delta p_{t.f}$ [Pa]	Relative error [%]
~ 500000	126,9	1,6
~ 850000	126	0,8
~ 1000000	125,4	0,3
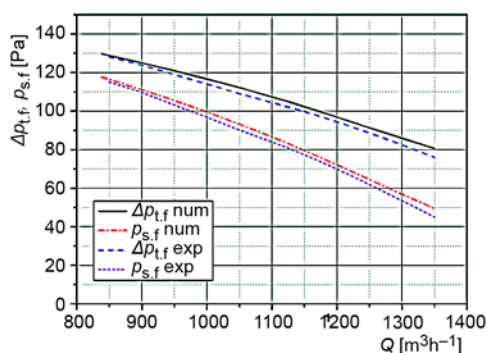
Figure 4. Axial-flow fan operating pressure curve (obtained numerically and experimentally)

Grid independence test

In order to cut the computational time (of numerical simulations), and at the same time to ensure the reliability of the obtained results too, first the grid independence test has been done, tab. 2. This test shown a very good accuracy for all three given discretization meshes, and there was no need to simulate the one with the largest number of mesh elements (~10^6 elements). The mesh with approximately 850000 elements was chosen as the best solution, obtaining result error less than 1%.

Validation of numerical results

The overall fan characteristics, primarily the total pressure of the fan ($\Delta p_{t.f}$) and the static pressure of the fan ($p_{s.f}$) are obtained, as the result of numerical simulations. In the validation process, numerical and experimental results are compared and shown in fig 4. The conclusion is that these results are in a very good agreement, with a relative error less than 3%, for the whole area of operating flow rates. Such accuracy can be attributed to more detailed modeling of the fan geometry (impeller and flat hub geometry). Also, the test chamber creates virtually the same conditions as they were during laboratory measurements. The CFD evaluates the hydraulic torque, and, therefore, the hydraulic efficiency is estimated according to following equation (which will be used in the next section):

$$\eta_h = \frac{Q\Delta p_{t.f}}{2\pi n T_{hyd}}, \text{ where } n \text{ [s}^{-1}] \tag{26}$$

Numerical results and discussion

Numerical simulations of flow in the axial-flow fan were conducted for four different air temperatures, 20 $^{\circ}$C, 50 $^{\circ}$C, 80 $^{\circ}$C, and 110 $^{\circ}$C. The obtained results are compared for different flow parameters.

First of all the operating characteristics of fan operating at air temperature of 20 $^{\circ}$C, obtained for the range of velocity flow rates, are compared with experimentally obtained operating curve, for the purpose of result validation, fig. 4. Further, the numerous numerical simulations have been performed, for different air temperatures and the similar range of velocity flow-rate.

Figure 5. Hydraulic efficiency of fan operating with different air temperatures

The hydraulic fan efficiencies for the range of fan operating volume flow rate, obtain by numerical simulations of flow in the fan, at different air temperatures (20 $^{\circ}$C, 50 $^{\circ}$C, 80 $^{\circ}$C, and 110 $^{\circ}$C) are presented in fig. 5. The hydraulic efficiencies are approximately the same, and slightly decreases by increasing the air temperature.
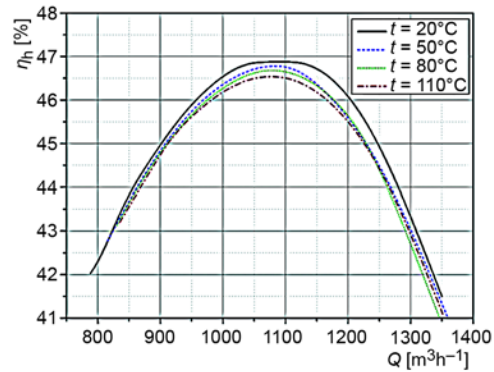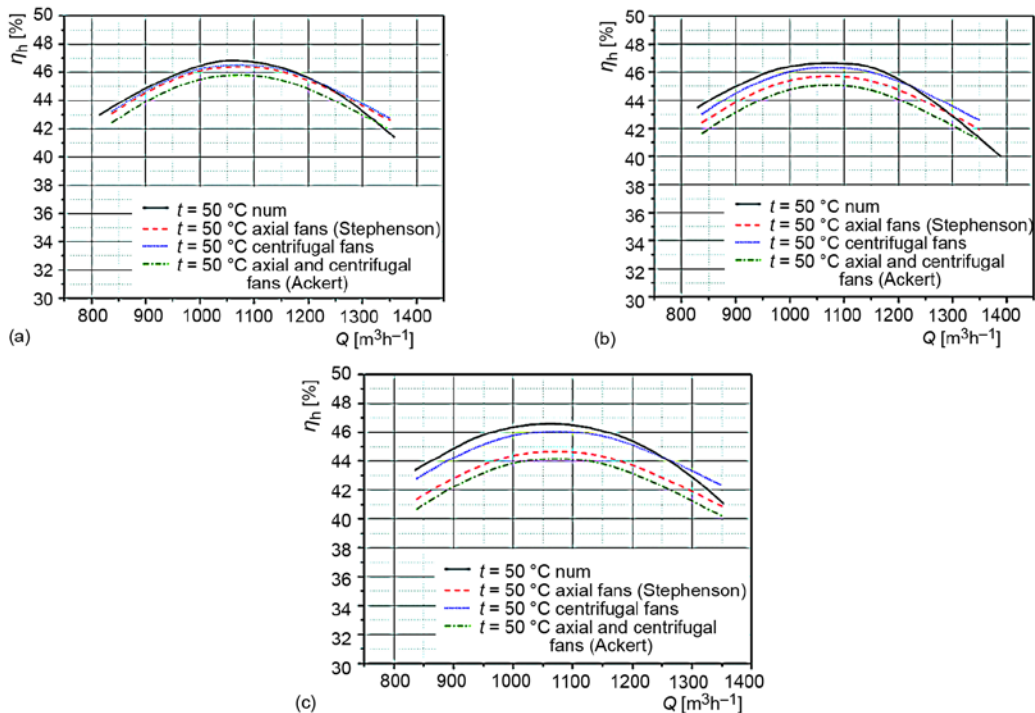

Figure 6. Hydraulic efficiency of the fan obtained numerically and by recalculation, eqs. (19) and (20), for different temperature; (a) $t = 50$ °C, (b) $t = 80$ °C, and (c) $t = 110$ °C

With higher temperatures of the air, the greater are the differences in outcome results for obtained numerically and calculated values of fan hydraulic efficiencies, obtained by the

S1444

Bogdanović-Jovanović, J. B., *et al.*: Performance of Low-Pressure Fans …
THERMAL SCIENCE, Year 2016, Vol. 20, Suppl. 5, pp. S1435-S1447

proposed eq. (19) for axial-flow fans. Also, hydraulic efficiencies for all given temperatures were calculated using eqs. (18) and (20), event tough eq. (18) is valid for centrifugal fans. Surprisingly, eq. (18) agrees better with the numerical simulation results, shown in fig. 6.

Due to unfavorable hub shape, the efficiency is very low comparing to machines of this type.

As previously shown in the paper, the equations for the conversion of fan operating regimes are used for recalculation of fan parameters, considering the change of fan geometrical parameters, fan rotational speed and gas (air) operating characteristics. In this case, only air temperature differs from case to case, therefore eq. (24) can be used for recalculation of operating parameters. The comparison of operating curves obtained in such recalculation (taking into account changing of hydraulic efficiency) and using numerical simulations, are presented in figs. 7 and 8. Considering the change of hydraulic efficiency proposed by eq. (19) for axial-flow fans, obtained pressure curves are compared with numerically obtained pressure curves, shown in fig. 7.
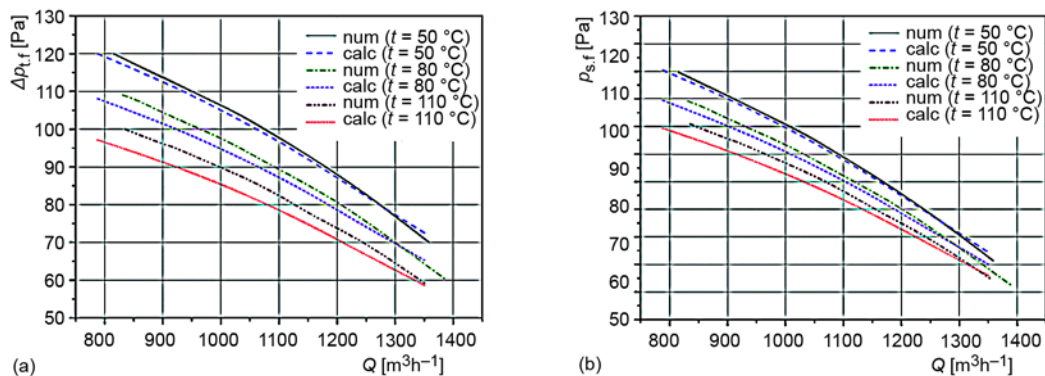

Figure 7. Comparison of pressure curves for different air temperatures obtained numerically and using eqs. (24) and (19); (a) total pressure curves, (b) static pressure curves

Using the eq. (18), which is primarily obtained for centrifugal fans, for operating flow rates near the optimal parameters of the fan calculated pressure curves are presented in fig. 8, showing better agreement than using eq. (19).
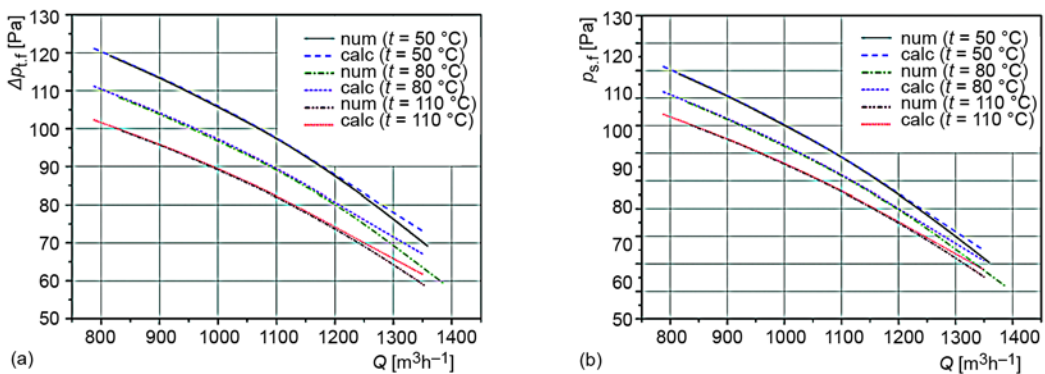

Figure 8. Comparison of pressure curves for different air temperatures obtained numerically and using eqs. (24) and (18); (a) total pressure curves, (b) static pressure curves

Total pressure and static pressure curves of the examined axial-flow fan obtained for different temperatures (50, 80, and 110 °C) are more strongly inclined for higher volume flow rates, compared to recalculated curves. Potential fan operating regimes for flow rates greater than 1250 m³/s indicate higher pressure differences, up to 7%, when calculated by eq. (18). A very similar situation occurs when neglecting the change of hydraulic efficiency.

Since the fan operating area for such large volume flow rates (larger than 1250 m³/s) is unfavorable from the point the fan efficiency, the both ways of obtaining fan operating curves, numerical or by recalculation eqs. (24), in the area of fan optimal performance (BEP), gives very similar results for all air temperatures.

The pressure and velocity distribution on the blade profiles was also obtained, and are shown for all considered temperatures for the mid-span (0,5) in fig. 9.
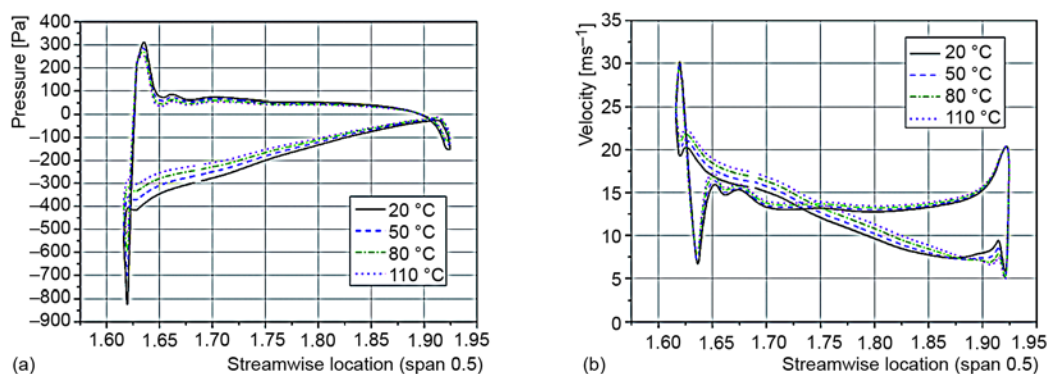

Figure 9. The pressure and velocity distribution for the mid-span blade profile, for volume flow rate
$Q = 1100$ **m³/s, when fan operates with different air temperatures**

Temperature distribution on the mid-span 0,5 cross-section of the fan runner is shown in fig. 10. It is noticeable that the temperature changing in the fan runner is about 0,5°. For all temperature cases, temperature distribution in the blade-to-blade view (mid-span) is similar.
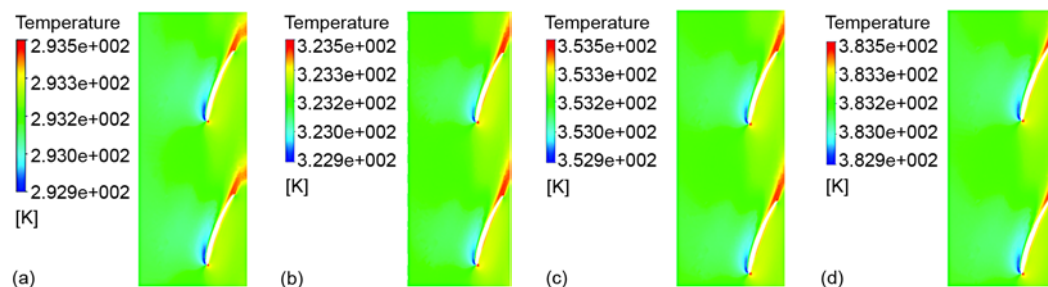

Figure 10. Temperature distribution for the mid-span blade profile for BEP of the axial-flow fan;
(a) $t = 20$ **°C, (b)** $t = 50$ **°C, (c)** $t = 80$ **°C, and (d)** $t = 110$ **°C** *(for color image see journal web-site)*

Conclusions

By increasing the air temperature, the air density decreases and the coefficient of kinematic viscosity increases. Furthermore, with the air temperature increasing, there is a

S1446

Bogdanović-Jovanović, J. B., *et al.*: Performance of Low-Pressure Fans …
THERMAL SCIENCE, Year 2016, Vol. 20, Suppl. 5, pp. S1435-S1447

possibility that the airflow in the fan is not in automodel field by the Reynolds number (fully turbulent flow, when the flow losses does not depend on Reynolds number). Then fan efficiency is not equal by the similarity law, and fan efficiency decreases with air temperature increasing.

With the air temperature increasing, numerically obtained maximum hydraulic efficiencies is almost the same value for all air temperatures, slightly lower and slightly shifted towards larger values of volume flow rates.

In this paper formulas for recalculation of low-pressure and mid-pressure fan operating characteristics, with regard to the air temperature change in at the fan inlet, are presented. There are also suggested different formulas for fan efficiency correction (when fan operate in regimes with $\mathrm{Re}u < \mathrm{Re}u^{(cr)}$). Comparing hydraulic efficiencies obtained by numerical simulations and using empirical formulas (for different air temperatures), one can notice that with the increase in air temperature, the larger is the difference of the obtained hydraulic efficiencies.

Numerical simulations of flow in one low-pressure axial-flow fan are carried out, for different air temperatures, showing satisfying results comparing to experimental results obtained for axial-flow fan operating with air at normal flow condition. Numerical simulation results of the axial-flow fan operating parameters with different air temperatures show a good agreement with results obtained by recalculation of flow parameters for the fan operating at air temperature of 20 °C, especially near BEP.

Using the recommended formula for axial-flow fans, the smaller the difference in the air temperature, the lower is the resulting difference of operating parameters. The maximum difference of obtained pressure values is up to 8% for maximal air temperature 110 °C.

Unexpectedly, using the correction formula for centrifugal fans efficiency leads to the pressure curves, which better suits the numerical simulation results. The numerical and calculated pressure curves differ significantly only for larger airflow rates, up to 7% (for $Q = 1350$ m^3/h).

Nomenclature

A – area, [m^2]
D – diameter, [m]
c – velocity, [ms^{-1}]
$\dot{m}$ – mass flow rate, [m^{3}kg^{-1}]
Ma – Mach number (= c/cs)
N – fan power, [W]
n – rotational speed, [s^{-1}, min^{-1} = rpm]
p – pressure, [Pa]
$\Delta p_{t.f}$ – fan total pressure, [Pa]
$p_{s.f}$ – fan static pressure, [Pa]
$p_{d.f}$ – fan dynamic pressure (or fan velocity pressure), [Pa]
Q – volume flow rate, [m^{3}s^{-1}], [Ls^{-1}]
r – radius, [m]
R – gas constant, [Jkg^{-1}K^{-1}]
t, T – temperature [°C, K], Torque, [Nm]

Greek symbols

β, β_d – correction coefficient due to compressibility, [–]
η – efficiency, [–]
κ – exponent of isentropic state change

ν – kinematic viscosity, [m^{2}s^{-1}]
Π – pressure ratio
ρ – density, [kgm^{-3}]
ω – angular velocity [s^{-1}]

Subscripts

d – dynamic quantities
e – external
ef – effectively
f – fan
h, hyd – hydraulic
i – internal
k – fan runner
nq – specific speed [–]
s – static quantities
t – total quantities
u – circumferential
I, II – inlet, outlet cross-section

Superscripts

cr – critical

Bogdanović-Jovanović, J. B., *et al.*: Performance of Low-Pressure Fans …
THERMAL SCIENCE, Year 2016, Vol. 20, Suppl. 5, pp. S1435-S1447

S1447

References

[1] Bogdanović, B., *et al.*, *Fans – Performance and Operating Characteristics* (in Serbian), Faculty of Mechanical Engineering Nis, Nis, Serbia, 2012

[2] Babić, M., Stojković, S., *Basics of Turbomachinery: Operating Principles and Mathematical Modeling* (in Serbian), University of Kragujevac, Scientific Paper, Belgrade, 1990

[3] Wallis, R. A., *Axial Flow Fans and Ducts*, Wiley Interscience Publications, New York, USA, 1983

[4] Solomahova, T. S., Cebejseva, K. B., *Centrifugal Fans* (in Russian), Mechanical Engineering, Moscow, 1980

[5] Eck, B., *Fans-Design and Operation of Centrifugal, Axial-Flow and Cross-Flow Fans*, Paramount Press, Oxford, UK, 1973

[6] Bogdanovic, B, *et al.*, Low-Pressure Axial Fan Designed with Different Specific Work of Elementary Stages, *Thermal Science, 16* (2012), Suppl. 2, pp. S605-S615

[7] Protić, Z., *et al.*, Novel Methods for Axial Fan Impeller Geometry Analysis and Experimental Investigations of the Generate Swirl Turbulent Flow, *Thermal Science, 14* (2010), Suppl. 1, pp. S125-S139

[8] Rajvanshi, A. K., Performance Estimation of an Axial Flow Fan, *IE(I) Journal-MC, 87* (2006), 2, pp. 34-37

[9] Oh, K., Kang, S., A Numerical Investigation of the Dual Performance Characteristics of a Small Propeller fan Using Viscous Flow Calculations, *Computers & Fluids, 28* (1999), 6, pp. 815-823

[10] Gabi, M., Klemm, T., Numerical and Experimental Investigations of Cross-Flow Fans, *Journal of Computational and Applied Mechanics, 5* (2004), 2, pp. 251-261

[11] Fortuna, S., Sobczak, K., Numerical and Experimental Investigations of the Flow in the Radial Fan, *Mechanics, 27* (2008), 4, pp. 138-143

[12] Bogdanović-Jovanović, J., *et al.*, Numerical Simulations and Performance Prediction of Low Pressure Fan, *Proceedings*, XIX Procesing 2006, SMEITS, Belgrade, 2006, pp. 75-80

[13] Lin, S. C., Huang, C. L., An Integrated Experimental and Numerical Study of Forward-Curved Centrifugal fan, *Experimental Thermal and Fluid Science, 26* (2002), 5, pp. 421-434

[14] Hotchkiss, P. J., *et al.*, Numerical Investigation into the Effect of Cross-Flow on the Performance of Axial Flow Fans in Forced Draught Air-Cooled Heat Exchangers, *Applied Thermal Engineering, 26* (2006), 2, pp. 200-208

[15] Stephenson, J. M., Efficiency and Drag of Axial-Flow Compressor Stage: The Connection Between the Efficiency of a Stage, the Forces on the Blade Sections and the Profile Drag; the Relation Between Different Definitions of Efficiency, and the Effect of other Sources of Loss, *Aircraft Engineering and Aerospace Technology, 25* (1953), 6, pp. 158-160

[16] ***, Inspection and Performance Fan Testing (VDI – Fan Regulation, in German), VDI-2044, pp. 36, 1966

[17] Stepanoff, A., J., *Turbo Blowers – Theory, Design and Application of Centrifugal and Axial Flow Compressors and Fans*, John Wiley & Sons, New York, USA, 1955

[18] Ferziger, J. H., Peric, M., Computational Methods for Fluid *Dynamics*, 3rd Rev. ed., Springer, Heidelberg, Germany, 2002

[19] Casey, M., Best Practice Advice for Turbomachinery Internal Flows, *QNET-CFD Network Newsletter (A Thematic Network For Quality and Trust in the Industrial Application of CFD), 2* (2004), 4, pp. 40-46